

CHARGE SEPARATION, VELOCITY SHEAR AND SUPPRESSION OF TURBULENCE AT A PLASMA EDGE IN THE FINITE GYRO-RADIUS GUIDING CENTER APPROXIMATION

M. Shoucri, G. Manfredi, P. Bertrand¹, A. Ghizzo¹, G. Knorr², J. Lebas¹,
E. Sonnendrucher¹, H. Burbaumer³, W. Entler³, G. Kamelander³ and E. Pohn³

Centre canadien de fusion magnétique, Varennes, Québec Canada J3X 1S1

¹ *LPMI-URA 835 CNRS, Université Henri Poincaré, Nancy, France*

² *Department of Physics and Astronomy, Univ. of Iowa, Iowa City, U.S.A.*

³ *Osterreichisches Forschungszentrum Seibersdorf, Austria*

1. Introduction

A 3D numerical gyro-kinetic code has been developed to study the existence and evolution of a charge separation at a plasma edge. The code includes the effect of a finite Larmor radius correction and polarization drift. The finite Larmor radius allows for a charge separation at a plasma edge to exist, and the polarization drift, which has different sign for ions and electrons, has a tendency to accentuate the charge separation in a time varying electric field and in the presence of strong gradients. We present first results obtained for the case of a Cartesian three-dimensional plasma layer, in which z represents the toroidal periodic direction, x represents the poloidal periodic direction, and y represents the radial direction. The direction of the magnetic field is very close to the normal z of the $x - y$ plane, and makes an angle $\theta = 89.5$ with the x axis (see Fig. 1).

2. The Pertinent Equations

The pertinent equations for the electrons are given by the gyro-kinetic equation:

$$\frac{\partial f_e}{\partial t} + \nabla \cdot (\vec{v}_{\perp e} f_e) + \vec{v}_{\parallel} \cdot \nabla_{\parallel} f_e \pm \vec{E}_{\parallel} \cdot \frac{\partial f_e}{\partial v_{\parallel}} = 0 \quad (1)$$

$$\vec{v}_{\perp e} = \vec{v}_D + \vec{v}_{pe}; \quad \vec{v}_D = \frac{\vec{E}^* \times \vec{B}}{B^2}; \quad \vec{v}_{p_{i,e}} = \pm \frac{m_{i,e}}{eB^2} \left[\frac{\partial \vec{E}_{\perp}^*}{\partial t} + (\vec{v}_D + \vec{v}_{\parallel}) \cdot \nabla \vec{E}_{\perp}^* \right] \quad (2)$$

The ions are described by fluid guiding center equations [1]:

$$\frac{\partial n_i}{\partial t} + \nabla \cdot (\vec{v}_{\perp i} n_i) = 0 \quad (3)$$

The motion of the heavy ions along the magnetic field is neglected.

Poisson equation:

$$\Delta\phi = -\frac{e}{\epsilon_0}(n_i^* - n_e^*) \quad (4)$$

The star is an abbreviation for an integral operator:

$$a^*(y) = \int_{-\infty}^{\infty} G(y-y')a(y')dy' \quad (5)$$

In Fourier space, this integral operation is equivalent to multiplying the coefficient of the mode $e^{i\vec{k}\cdot\vec{r}}$ by a factor $G_k = \exp(-k_{\perp}^2 \rho_{i,e}^2 / 2)$, $\rho_{i,e} = v_{ti,e} / \omega_{ci,e}$. As initial value, we take for the ions and electrons:

$$n_i(y) = N(y)(1 + \epsilon \sin k_0 x + \epsilon \sin 2k_0 x + \epsilon \sin 3k_0 x) \quad (6)$$

$$f_e(x, y, z, v_{\parallel}, t = 0) = \frac{N(y)}{\sqrt{2\pi T_e}} e^{-v_{\parallel}^2 / 2T_e} \quad (7)$$

$$T_{e0} = T_{i0} = 1, \quad m_i / m_e = 1840, \quad \omega_{ci} / \omega_{pi} = 0.9, \quad \rho_i / \lambda_{De} = 0.9$$

$$N(y) = \frac{1}{2} [1 + \tanh(1.6y)]; \quad T_e(y) = T_{e0} [0.2 + 0.4 \tanh(1.6y)] \quad (8)$$

We use a box with $L_x = 28$, $L_y = 12$ and $L_z = 150$, $k_0 = 2\pi/L_x$. The initial equilibrium is perturbed as indicated in Eq. (5) with $\epsilon = 0.002$. Equations (1-4) are solved using a method of fractional steps similar to what has been previously reported in Ref. [1]. The number of points used is $N_x N_y N_z N_v = 128 \times 128 \times 64 \times 128$.

3. Results

The low frequency waves associated with the inhomogeneous system we are studying are the Kelvin-Helmholtz instabilities which are driven by a gradient in the transverse velocity shear, and the drift waves associated with the gradient in the density [2].

Figure 2 shows the time evolution of the first four Fourier modes in the poloidal (x) direction. The second mode dominates at $t = 8500$. Indeed, the motion of the electrons along the magnetic field line (the presence of E_z), limit the growth with respect to what has been presented in Ref. [1] for 2D for the same parameters. Figure 3 shows the time evolution of the

first two modes in the toroidal z direction. There is a rapid growth of these modes after $t = 4000$. These modes saturates however at a relatively lower level compared to the modes in Fig. (2). The physics associated with the evolution of this system is essentially associated with the charge separation in the poloidal $x - y$ plane, and the drift mode associated with the z dependence [2]. With the shear in the velocity associated with the charge separation in the poloidal $x - y$ plane is associated the Kelvin-Helmholtz instability. The results we are presenting are the combined effects of the drift and the Kelvin-Helmholtz instabilities. Figure 4 shows the time evolution of the potential profiles (full curves) and the charge (dotted curves), spatially averaged over the periodic directions x and z . We note the potential profile evolving initially from a sine-like shape to a half-sine like shape, which then grows and saturates. The potential in Fig. 4 is reaching a level slightly higher than the equivalent results presented in Ref. [1]. This can be the effect of the combined velocity shear and drift instabilities present together after $t = 4000$. This can also be the effect of a small dissipation in the 3D code, since we are using only 64 points in the z -direction for $L_z = 150$. It has been shown [3,4] that a small dissipation in the present set of equations can have significant effect on the charge separation and the potential associated with the edge, and can significantly increase the velocity at the edge. We note also in the time evolution of the charge and in the potential in Fig. 4 an evolution more rapid than what has been presented in Ref. [1] for the case $\theta = 89.5^\circ$ (note in Ref. [1] we are plotting the negative value of the potential). Figure 5 shows the time evolution of the electric field profiles $E_y(y)$, spatially averaged over the periodic directions x and z ($v_{Dx} \sim E_y$). Finally Fig. 6 shows the profiles of the electron density, spatially averaged over the periodic directions x and z , (full curve) initially at $t = 0$ and at the end at $t = 8500$. Also shown is the equivalent smoothed ion density n_i^* (note that $n_i^* - n_e$ is the charge in Eq. 4 since the electron gyro-radius can be neglected; this charge is shown in dotted lines in Fig. 4). Work is in progress for further studies on this problem.

Acknowledgments

The CCFM is funded by Hydro-Quebec and the Institut national de la recherche scientifique.

References

- [1] G. Manfredi, M. Shoucri et al.: *accepted for publication in Physica Scripta* (1998).
- [2] M. Shoucri and G. Knorr: *Plasma Physics* **18**, 187 (1976).
- [3] M. Shoucri, G. Manfredi et al.: *submitted to J. Plasma Physics*.
- [4] M. Shoucri et al.: *Physica Scripta* **57**, 283 (1998).

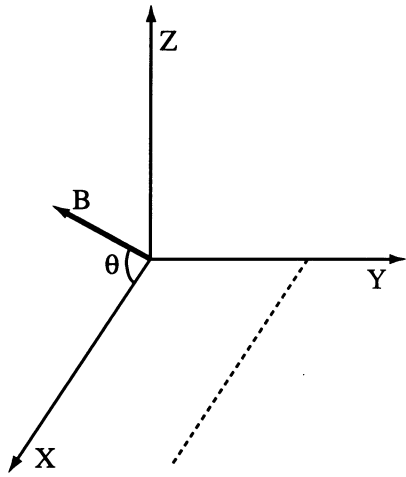


Figure 1

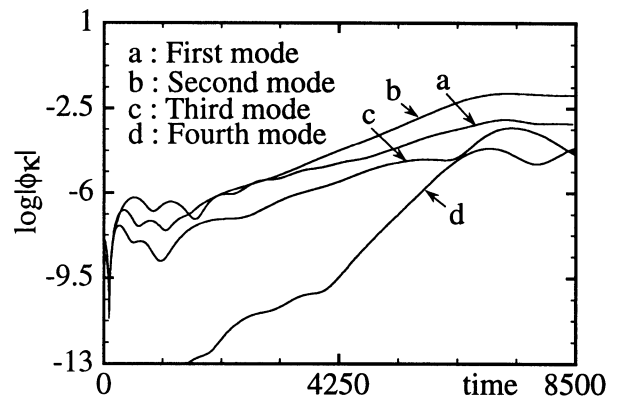


Figure 2

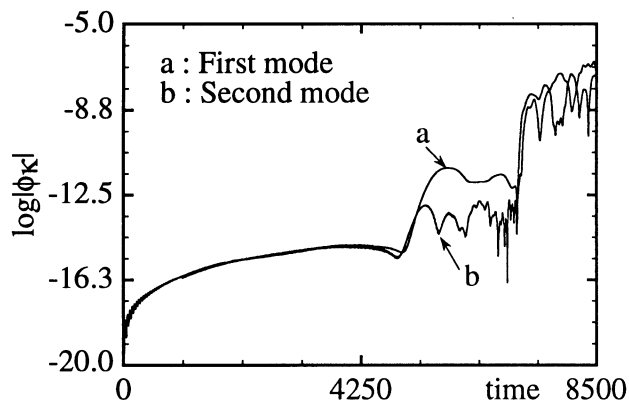


Figure 3

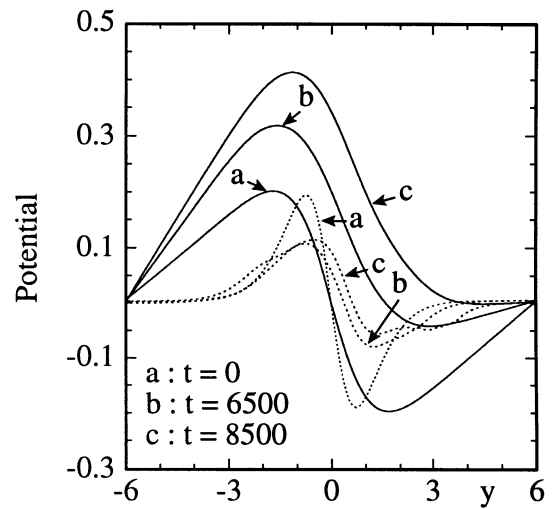


Figure 4

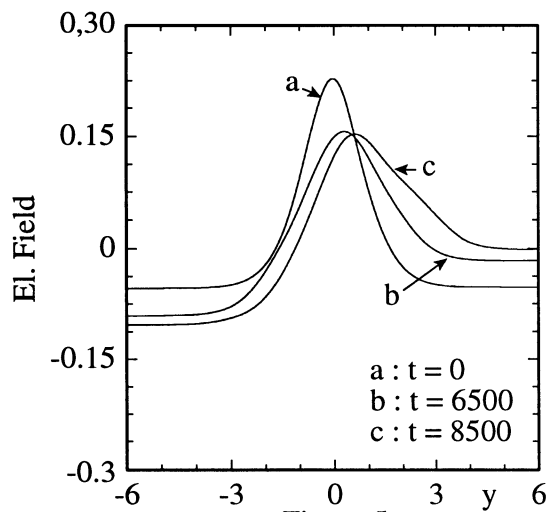


Figure 5

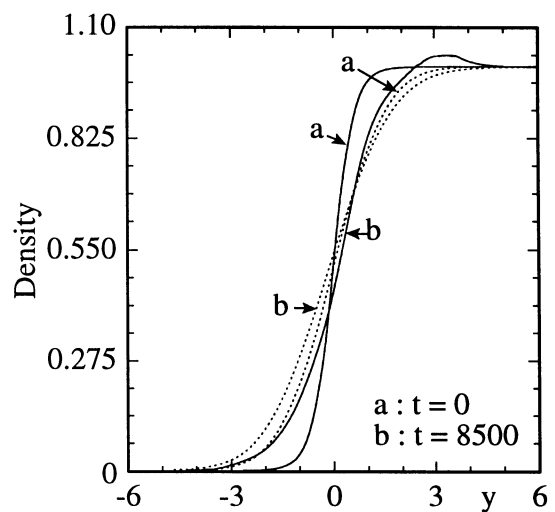


Figure 6